Electronic Supplementary Material (ESI) for Nanoscale.

Supplementary Information

Cellulose Nanofibers Derived Carbon Aerogel with 3D Multiscale Pore Architecture for High-Performance Supercapacitors

Lumin Chen[a], Houyong Yu [a]*, Ziheng Li[a], Xiang Chen[a], Wenlong Zhou[a]

[a]*National Engineering Lab for Textile Fiber Materials & Processing Technology, College of Textile Science and Engineering, Zhejiang Sci-Tech University, Hangzhou 310018, China*

*Corresponding authors. Tel: +86-571-86843618; Fax: +86-571-86843619.
E-mail addresses: phdyu@zstu.edu.cn

Electrochemical measurements

The electrochemical performance of electrodes was performed using a three-electrode system in an electrochemical workstation (CHI660E, CH Instruments Ins., USA). A saturated calomel electrode (SCE), platinum wire, and 1 M H_2SO_4 were used as the reference electrode, the counter electrode, and the electrolyte, respectively. The Cyclic voltammetry (CV) tests were carried out in a scan rate range of 10-600 mV s^{-1} with a potential window of 1.6 V. Galvanostatic charge-discharge test was performed between -0.4 and 1.2 V at current densities of 1-30 A g^{-1}. The electrochemical spectroscopy (EIS) measurements were conducted in a frequency range of 0.01-100 kHz with an AC amplitude of 5 mV at open circuit potential. The electrochemical tests of symmetric supercapacitors were performed in a two-electrode system.

For three-electrode system, the specific capacitances (C_s) can be calculated from CV via the following equation (1):

$$C_s = \frac{Q}{mS\Delta V} \quad (1)$$

Where Q is the integrated area of CV curve, m is active material mass, S is the scan rate of CV curve, ΔV is the potential window.

or from GCD curve by the equations (2):

$$C_s = \frac{It}{m\Delta V} \quad (2)$$

Where I is the discharge current, t is the discharge time, m is active material mass, ΔV is the voltage after IR drop, respectively.

For two-electrode system, the areal specific capacitances (C_A in mF cm^{-2}) and

gravimetric specific capacitances (C_g in F g^{-1}) can also be calculated by the following equations:

$$C_A = \frac{It}{S\Delta V} \quad (3)$$

$$C_g = \frac{It}{m\Delta V} \quad (4)$$

Where I is the discharge current, t is the discharge time, S is the area of the hydrogel electrode, m is active material mass of two electrodes, ΔV is the voltage after IR drop. The areal energy density E_A (mWh cm^{-2}) and power density P_A (mW cm^{-2}) were obtained from the following equations:

$$E_A = \frac{1}{2} \times C_A \times \frac{\Delta V^2}{3.6} \quad (5)$$

$$P_A = \frac{3600 \times E_A}{t} \quad (6)$$

Where C_A, ΔV and t are the areal specific capacitances of supercapacitor, the voltage after IR drop and discharge time, respectively.

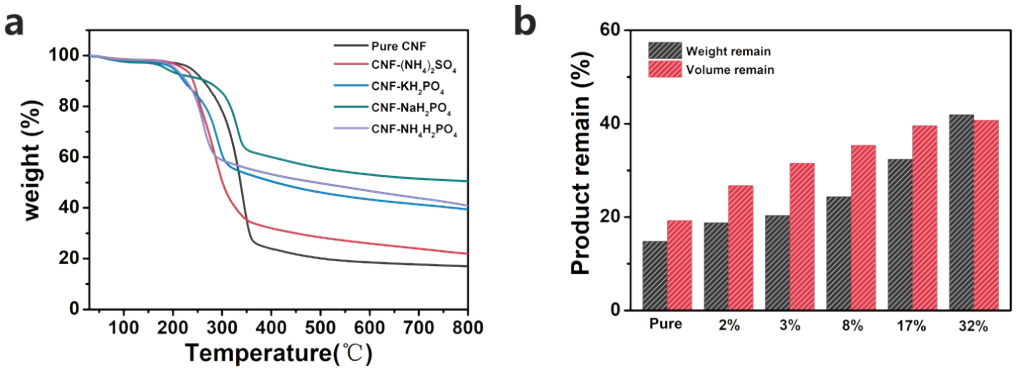

Figure S1. (a) TG curves of pure CNF and CNF soaked with $(NH_4)_2SO_4$, KH_2PO_4, NaH_2PO_4, and $NH_4H_2PO_4$. (b) Weight and volume remain of CNFAs prepared by carbonization from pure CNF and CNF soaked with different amounts of NaH_2PO_4.

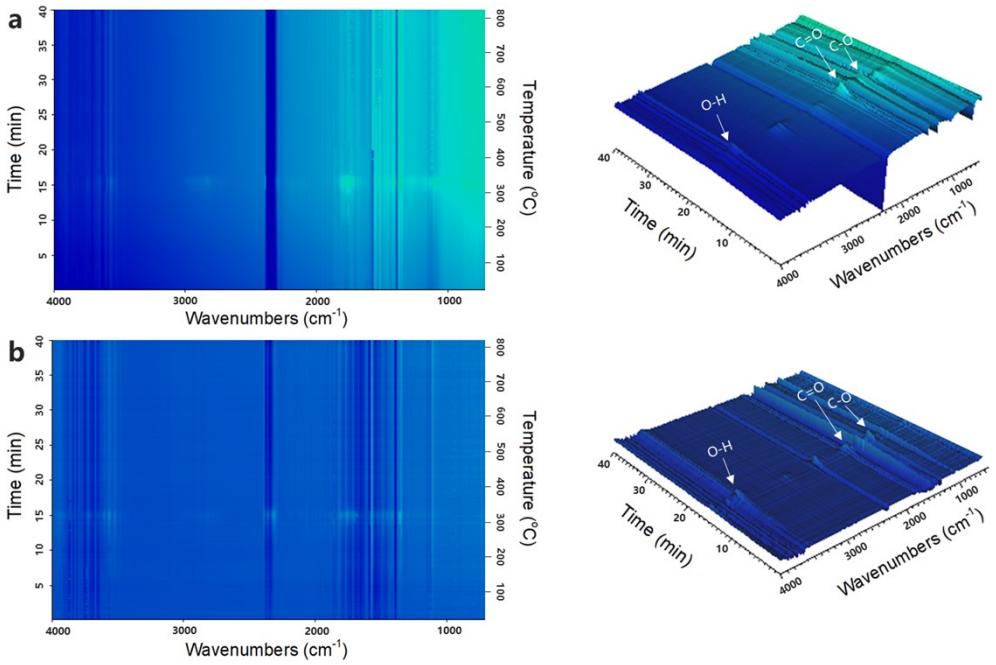

Figure S2. 3D FTIR spectra of (a) pure CNF and (b) CNF-32 wt% NaH_2PO_4 composite.

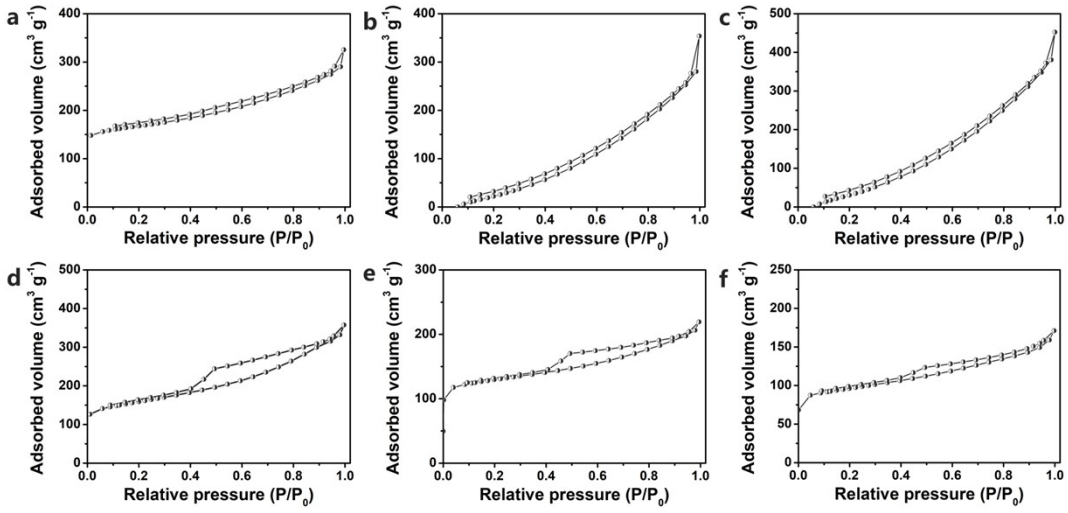

Figure S3. Nitrogen adsorption-desorption isotherm of (a) pure CNFAs, (b) CNFAs-2%，(c) CNFAs-3%，(d) CNFAs-8%, (e) CNFAs-17%，and (f) CNFAs-32%.

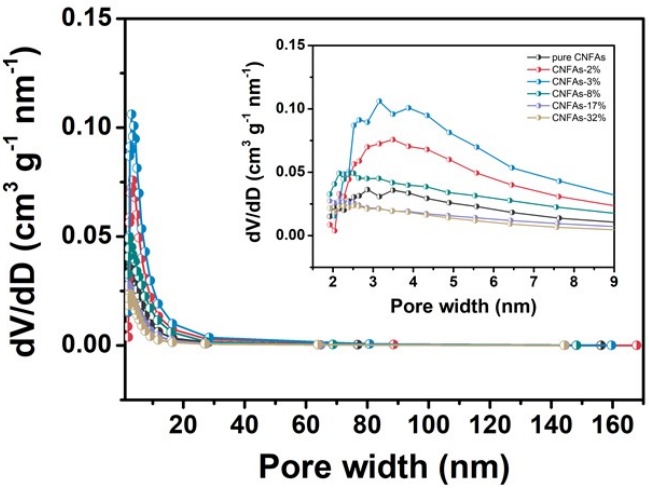

Figure S4. The pore-size distribution of CNFAs.

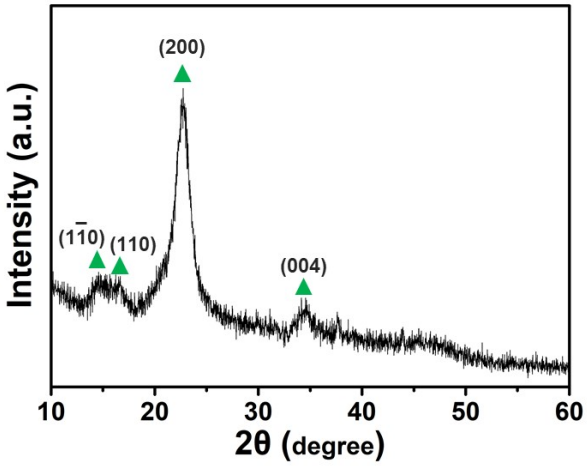

Figure S5. The XRD pattern of CNF.

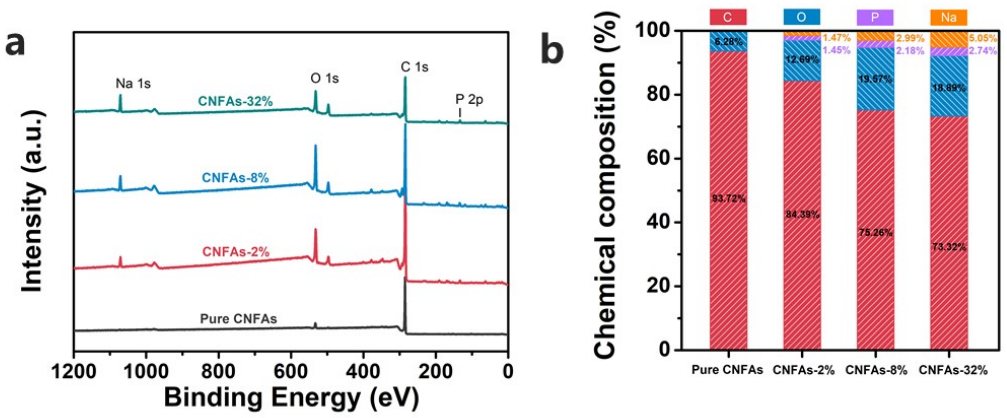

Figure S6. (a) XPS survey spectra of pure CNFAs, CNFAs-2%, CNFAs-8%, and CNFAs-32%. (b) The chemical composition content of pure CNFAs, CNFAs-2%, CNFAs-8%, and CNFAs-32% derived from XPS results.

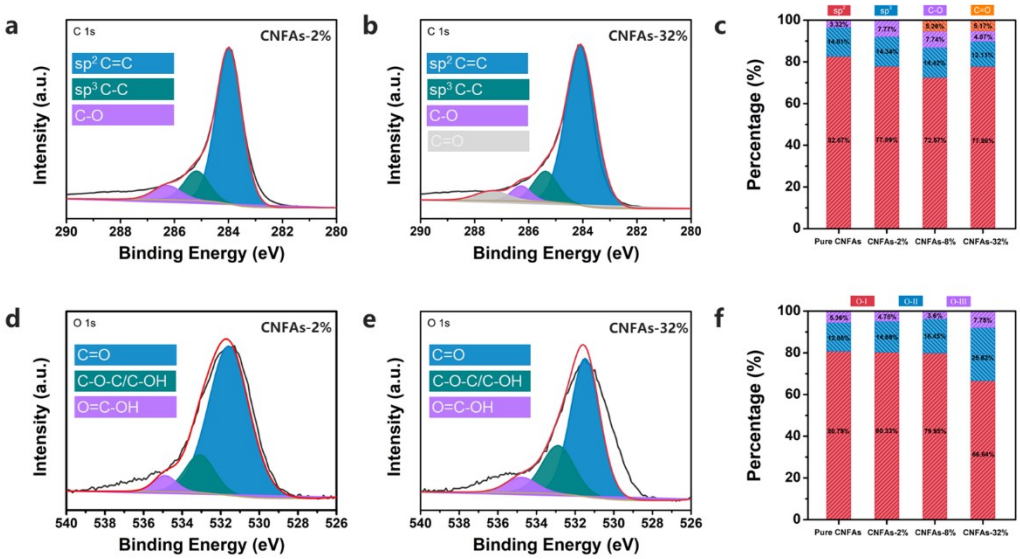

Figure S7. C 1s XPS spectra of (a) CNFAs-2% and (b) CNFAs-32%. (c) The functional group content of pure CNFAs, CNFAs-2%, CNFAs-8%, and CNFAs-32% derived from C 1s XPS spectra results. O 1s XPS spectra of (d) CNFAs-2%s and (e) CNFAs-32%. (f) The functional group content of pure CNFAs, CNFAs-2%, CNFAs-8%, and CNFAs-32% derived from O 1s XPS spectra results.

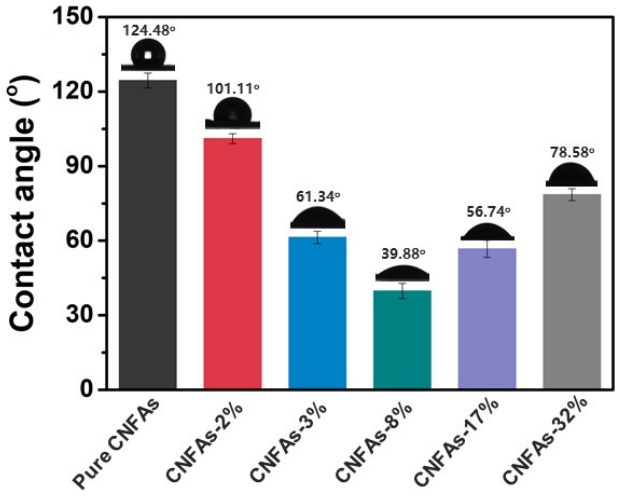

Figure S8. Water contact angle values of CNFAs.

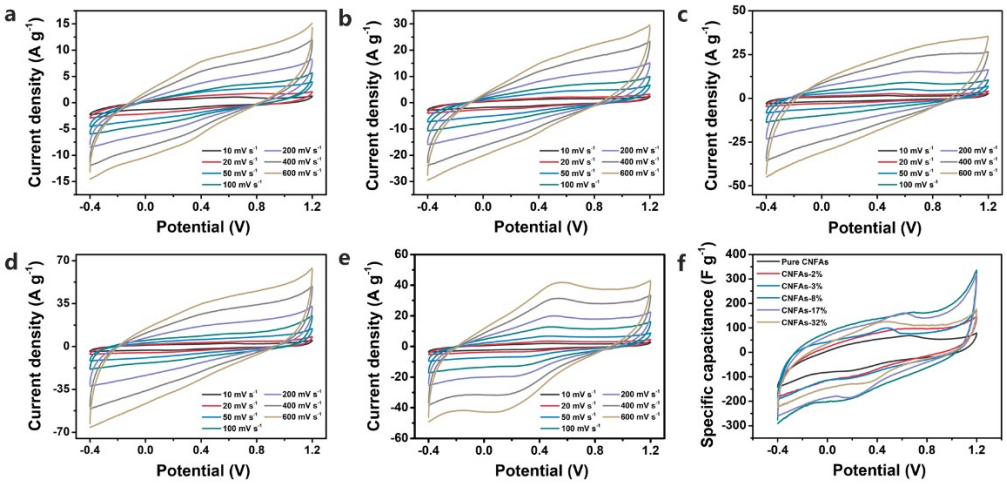

Figure S9. CV curves of (a) pure CNFAs, (b) CNFAs-2%, (c) CNFAs-3%, (d) CNFAs-17%, and (e) CNFAs-32% at different scan rates. (f) CV curves of the six samples at a scan rate of 10 mV s^{-1}.

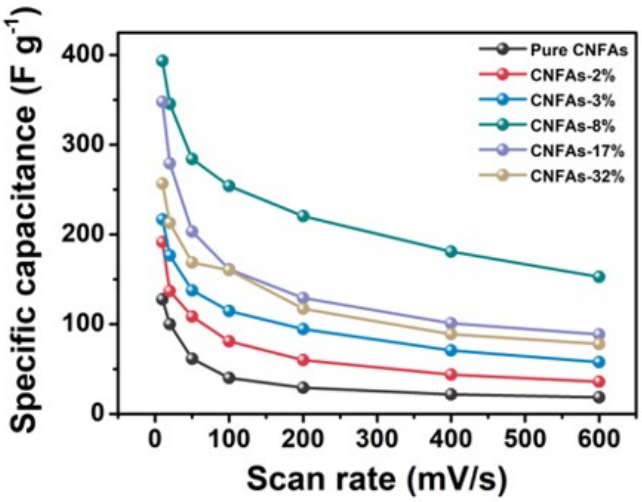

Figure S10. Specific capacitance of pure CNFAs, CNFAs-2%, CNFAs-3%, CNFAs-8%, CNFAs-17%, and CNFAs-32% at different scan rates.

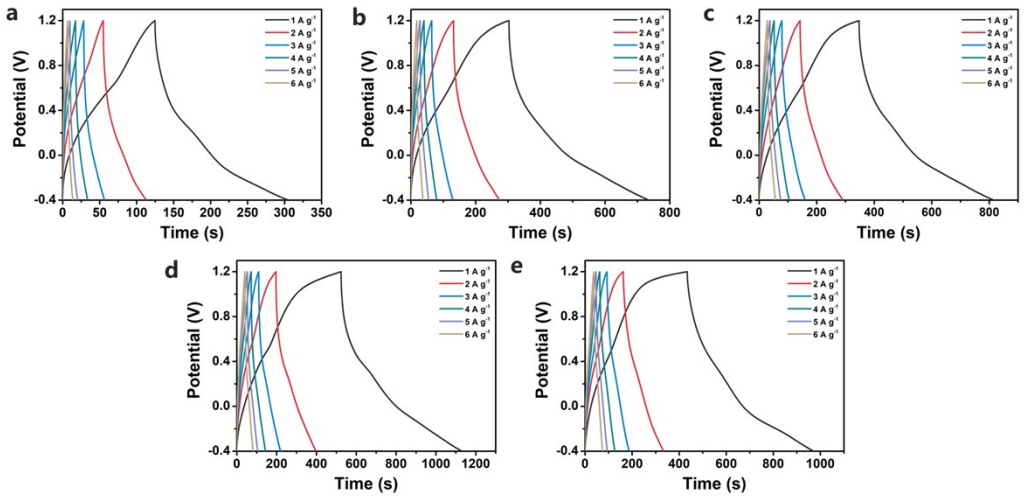

Figure S11. GCD curves of (a) pure CNFAs, (b) CNFAs-2%, (c) CNFAs-3%, (d) CNFAs-17%, and (e) CNFAs-32% at different current densities.

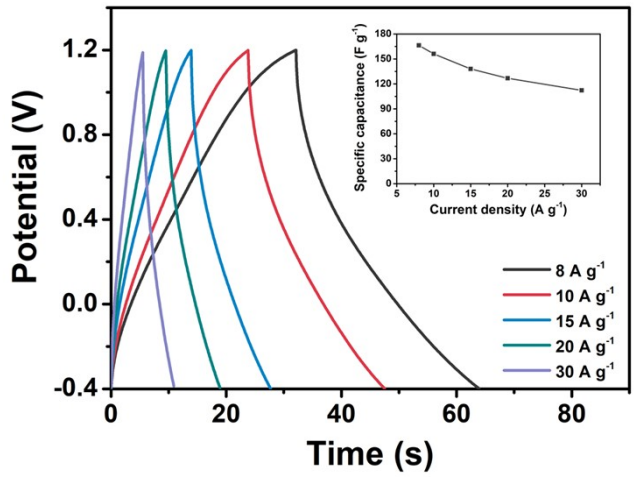

Figure S12. GCD curves of CNFAs-8% electrode at different current densities, the inset shows the corresponding specific capacitance.

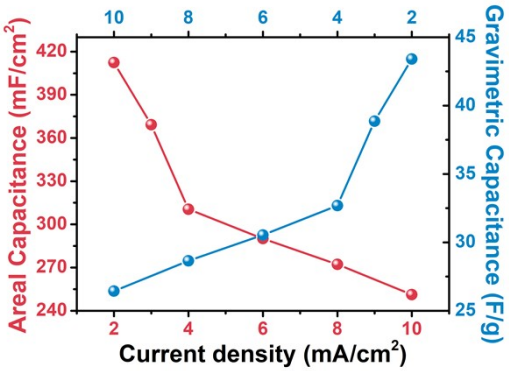

Figure S13. Variation of areal capacitances and gravimetric capacitances at different current densities.

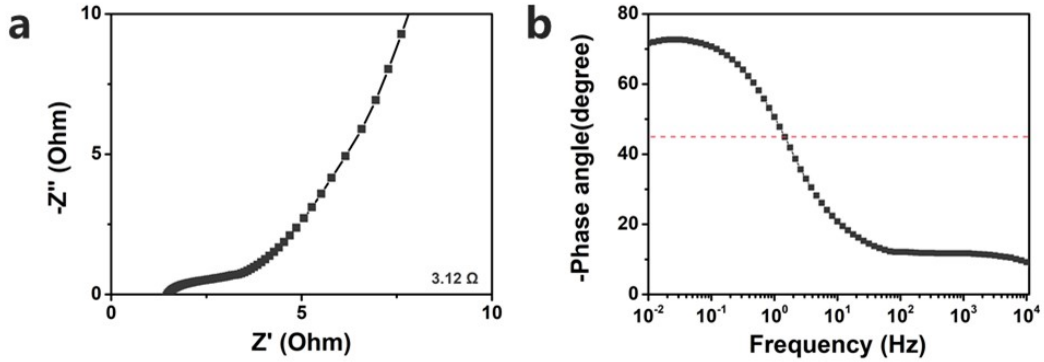

Figure S14. (a) Nyquist plot and (b) bode plot of CNFAs-8% // CNFAs-8% symmetric supercapacitor.

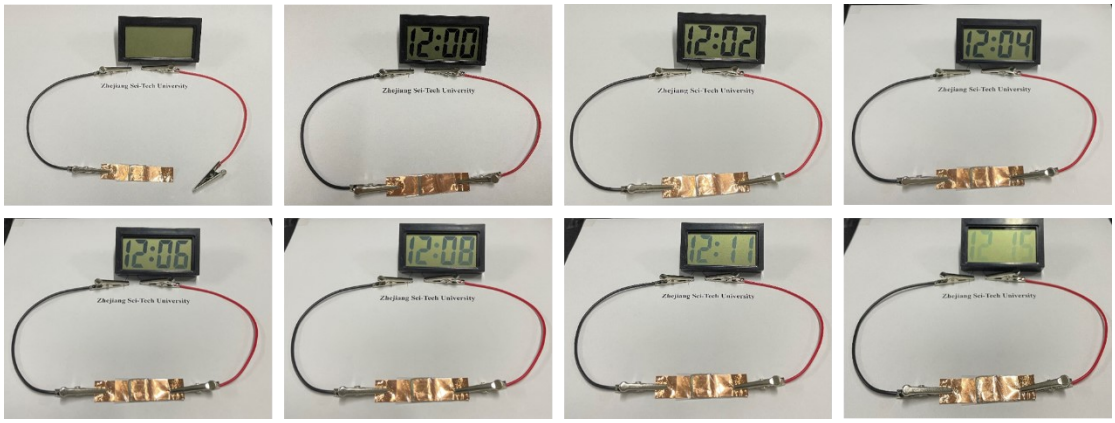

Figure S15. Photographs of electronic watch powered using CNFAs-8%//CNFAs-8% symmetric supercapacitor.